

Disturbance Observer-Based Intelligent Control for Trajectory Tracking in Redundant Robotic Manipulators

Mohammed H. Al-Mola^{a,1,*}, Sherif I. Abdelmaksoud^{b,2}

^a Department of Agricultural Machines and Equipment, College of Agriculture and Forestry, University of Mosul, 41002 Mosul, Nineveh, Iraq

^b Mechatronics Department, New Cairo Technological University, Cairo, Egypt

¹ dr.mohammedalmola@uomosul.edu.iq; ² eg.sherif89@gmail.com

* Corresponding Author

ARTICLE INFO

Article history

Received May 05, 2025

Revised June 18, 2025

Accepted July 19, 2025

Keywords

RR Robotic Arms;

PID Controller;

Sliding Mode Control (SMC);

Active Force Control (AFC);

Disturbances;

Integral Square Error (ISE)

ABSTRACT

Redundant robotic manipulators require advanced control strategies to maintain stability and precision in the presence of dynamic disturbances. This study proposes an intelligent control scheme integrating Active Force Control (AFC) with a Proportional–Integral–Derivative (PID) controller to enhance the performance of a two-degree-of-freedom (2-DOF) robotic manipulator. The proposed AFC-PID controller is designed to suppress the effects of external disturbances, including torque noise. Comparative simulations demonstrate that the AFC-PID approach outperforms the conventional PID controller, providing improved stability and tracking accuracy in both manipulator links. Moreover, it compared with the Sliding Mode Control (SMC) control to verify the efficiency of the proposed controller. Quantitatively, the Integral Square Error (ISE) improvements compared to PID for link 1 and link 2 are 82.83% and 65.57%, respectively. Under disturbance conditions, performance gains are also observed, with ISE reductions of 86.2% and 65.36% for links 1 and 2. These results confirm the robustness and effectiveness of the proposed controller in maintaining consistent performance under challenging conditions. This is a significant improvement, reflecting the superiority over the conventional systems.

This is an open-access article under the CC-BY-SA license.



1. Introduction

Two-link RR manipulators, distinguished by their dual revolute joint architecture, constitute a fundamental and widely studied configuration in the field of robotic systems due to their structural simplicity, analytical tractability, and relevance to a broad range of motion control applications. Due to their structural advantages and adaptability, they play a vital role in a wide range of robotic applications. Improving performance and accuracy of sophisticated production processes or micromanipulation case can be accomplished using the degrees of freedom of such manipulators. To describe the motion of dynamic systems with two degrees of freedom, two independent coordinates are needed. T-stability is a necessary condition for stability under that situation. Thus, multi-degree-of-freedom robotic manipulators behave, in general, and for simplification of analysis, they are represented as degrees-of-freedom robotic manipulators. Studies have focused on the development of robot software, hardware, and behavior to improve performance. The conducted an evaluation of social robot design trends in order to provide an evidence-based methodology and recommendations

that could stimulate additional social robot development [1]. Social robots are being utilized more and more in public areas to engage with people and provide first-line customer service. Furthermore, they discovered a significant correlation between the adoption of social robots for crisis management and their acceptance in societal crises [1]-[2]. The widespread use of social robots in retail stores and shopping malls is a clear indication of the propensity to feel good. Fuzzy logic controllers frequently draw from human business experience.

In many control and rehabilitation systems, the technique known as active force control (AFC) is used as Adaptive Disturbance Compensation. Implementing force control is necessary to provide feedback and adjust forces based on preset criteria. This technique has been used in shoulder rotation rehabilitation to improve shoulder range of motion by using a haptic device to reflect a force on the user's hand [3]. To improve ride comfort, active force control has also been used in Underwater Remotely Operated Vehicle [4], brake systems [5], [6], and seat suspension systems to adjust the damping force of semi-active control devices [7]. Enhancing tracking accuracy and decrease model uncertainty, active force control has been also applied to upper limb training with functional electrical stimulation in the field of stroke rehabilitation [8]. Active force control has also been applied to aerial manipulation platforms for interaction control and planning [9], to provide intentional and controlled contact with unstructured environments. Integrating control mechanisms into these robotic systems adds the advantage of eliminating human effort in monitoring the motor system, leading to the development of robotic arms capable of adapting and automatically correcting their trajectories [10]. Several control methods have been explored for robotic manipulators, including PID control [11]-[13], fuzzy logic control (FLC) [14], artificial neural network (ANN) control [15], and optimal algorithm using PSO with PID controller [16]. These approaches have been analyzed in terms of their benefits and limitations when coupled with a conventional PID controller [17]. A self-tuning proportional derivative controller has been applied to a two-link robot system [18], integrating PID gains with sliding mode control (SMC) [19], [20], and using feedback linearization based on sliding mode control (FLSM) for a four-degree-of-freedom (4DOF) robot arm to enhance stability [21]. Fuzzy logic controllers have been used to adjust PID gains dynamically, reducing system feedback errors [22]. Active force control (AFC) techniques have been employed to optimize PID controller gains, including experimental integration with iterative learning algorithms [5], [23]. AFC is widely used in robotic manipulators to regulate applied forces during interaction with the environment. Various studies have examined AFC strategies in robot manipulators, comparing PID control with Active Disturbance Rejection Control (ADRC) for position and velocity regulation in two-DOF robots [24]. Additionally, force and impedance controllers have been proposed for robotic manipulators to reduce vibration [25]. A method for virtual robotic manipulator control with force feedback has been introduced for virtual environments [26]. These existing approaches highlight the need for an integrated disturbance compensation framework to enhance stability and adaptability in RR manipulators.

Many researches have revealed that AFC is an important control system approach. It has shown impressive results in the deployment of Underwater Remotely Operated Vehicles (UROV) both for direct operational and exploratory tasks built on Evolutionary Computation (EC) models [4]. Additionally, AFC has been employed for high-precision robotic assembly without surface-dependent calibration and has been successfully used for assembly across a wide range of surface stiffness [27]. Further, AFC has been applied to an inverted pendulum system along with a PID control approach, and it performed better than traditional PID controllers, improving stability and minimizing overshoot in the system response [28]-[29]. Further, AFC outperforms pure PID controllers, particularly with disturbances when applied to suppress liquid sloshing in a two-degree-of-freedom liquid container transfer system [30], and three degrees-of-freedom planar robots [31], sliding mode-PID [32]. Using proportional-derivative (PD) control and sliding mode control (PD) with sliding mode control in quadrotor trajectory tracking [33], [34]. Recently, a number of control methods have been proposed, such as PID control with disturbance loads [6], [35]-[38], adaptive control [39], robust control to overcome the chatter phenomenon that occurs during satellite acquisition in the rotating device [40], and PID merging with Coot Optimization Algorithm to improve robustness toward

disturbances [41]. Other studies highlighted a variety of external disturbances implemented in two-link robotic manipulators, including sinusoidal and white noise, random torque fluctuations, and pulse-width modulated signals that impacted the behavior of links stability [42]-[44]. Unmodeled dynamics, actuator-driven instabilities, and periodic forces disturbances that need to damp in the system to obtain the robustness [45]-[47]. Addressing external uncertainties, bounded disturbances, and input constraints necessitates enhanced PID tuning for consistent performance under dynamic conditions [48]-[50]. These findings underscore the necessity for enhanced PID designs, integrating adaptive and robust techniques to mitigate the diverse disturbance effects encountered in two-link robotic manipulators. In order to obtain an optimal control. To model some of the realistic disturbances faced by robotic arms, several examples of these disturbances are presented. For example, periodic vibrations resulting from the rotary actuators in robot arms or their main bases in factories can be translated into a sine wave, affecting the joints and their motion stability. Similarly, sudden shocks that accompany robotic arm movement, such as sudden collisions or rapid stops, can be represented as pulsating disturbances. On the other hand, there are external disturbances that can be represented as band-limited noise, such as wind or any external force that negatively affects the arm's motion during movement. All of these types of external disturbances, and others, pose a constant challenge to the movement performance of two-jointed robots. Therefore, they require control systems capable of adapting the arms to dampen and absorb these disturbances, such as the proposed technique for maintaining stable motion performance [28]-[29].

However, the primary contribution of this study is the development and implementation of a hybrid control strategy that integrates the conventional Proportional-Integral-Derivative (PID) controller with the Active Force Control (AFC) technique. This combination aims to significantly improve the motion accuracy and trajectory tracking capabilities of two-link RR manipulators, especially under the influence of external disturbances. By harnessing the simplicity and fast response of PID control in tandem with the robustness and disturbance-rejection strengths of AFC, the proposed method enhances both the stability and directional control of the manipulator system. Furthermore, a comprehensive comparative analysis is conducted against control approaches to quantitatively evaluate the performance, demonstrating the superiority of the proposed hybrid scheme in maintaining precise control in challenging operational conditions.

The work can be separated into three parts: Section 2, the dynamic model of the system, the governing equation as well as the control methods; PID, SMC, and AFC technique which are used in the design of the proposed control. Section 3 presents and analyses the comparison study. Section 4 concludes with the conclusion.

2. Manipulator Dynamics Model

The Dynamic analysis of robots focuses on understanding the relationship between the torques applied to the joints of robots or the forces generated by rotational joint drives and the resulting motion, particularly how to accelerate the arms, how much velocity need for the arms to respond, and the arms position. This analysis is crucial for the design and implementation of effective control systems. However, achieving precise and reliable control might be challenging due to the inherently complex and highly non-linear dynamics exhibited by robotic manipulators. These nonlinearities introduce unique difficulties in evaluating the accuracy and robustness of various control schemes. Fig. 1 displays the configuration of a vertical two-degree-of-freedom (2DOF) robotic arm, which serves as a representative model for dynamic analysis and control evaluation. The two-link flexible robot manipulator may be characterized as in [6], [27], and [38] if friction or potential disturbances are not taken into account. To determine the center of mass for the two links, need to use the forward kinematics:

$$x_1 = L_1 \cos(\theta_1) \quad (1)$$

$$y_1 = L_1 \sin(\theta_1) \quad (2)$$

$$x_2 = L_1 \cos(\theta_1) + L_2 \cos(\theta_1 + \theta_2) \quad (3)$$

$$y_2 = L_1 \sin(\theta_1) + L_2 \sin(\theta_1 + \theta_2) \quad (4)$$

The velocity is obtained by differentiating position with respect to time.

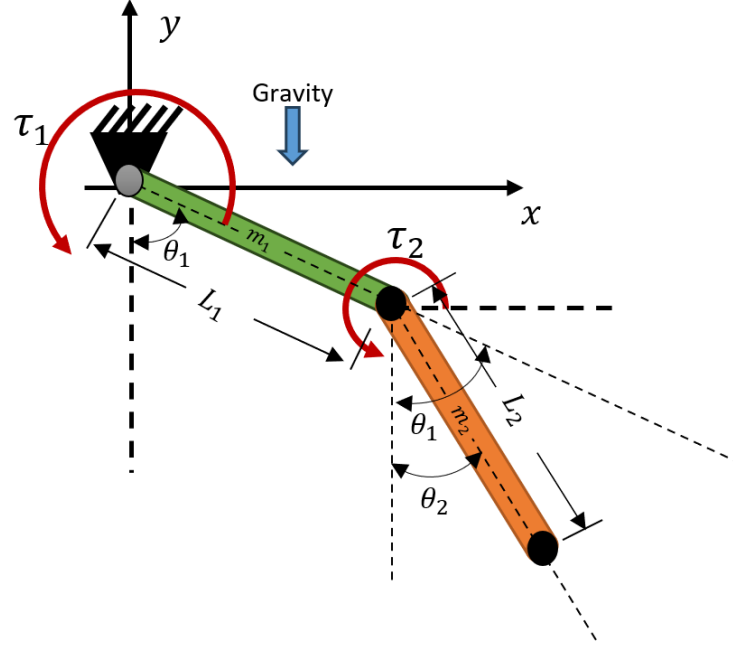


Fig. 1. Two-link RR joint configuration

$$\begin{aligned} \dot{x}_1 &= -(L_1 / 2) \sin(\theta_1) \dot{\theta}_1, \\ \dot{y}_1 &= (L_1 / 2) \cos(\theta_1) \dot{\theta}_1, \end{aligned} \quad (5)$$

$$v_1^2 = \dot{x}_1^2 + \dot{y}_1^2 = (L_1 / 2)^2 \dot{\theta}_1^2$$

$$\begin{aligned} \dot{x}_2 &= L_1 \sin(\theta_1) \dot{\theta}_1 - (L_2 / 2) \sin(\theta_1 + \theta_2) (\dot{\theta}_1 + \dot{\theta}_2), \\ \dot{y}_2 &= L_1 \cos(\theta_1) \dot{\theta}_1 + (L_2 / 2) \cos(\theta_1 + \theta_2) (\dot{\theta}_1 + \dot{\theta}_2), \\ v_2^2 &= \dot{x}_2^2 + \dot{y}_2^2 \end{aligned} \quad (6)$$

Each link has translational and rotational kinetic energy, and can be calculated as:

$$KE = \frac{1}{2} m_1 v_1^2 + \frac{1}{2} m_2 v_2^2, \quad (7)$$

$$KE = \frac{1}{2} m_1 (L_1 / 2)^2 \dot{\theta}_1^2 + \frac{1}{2} m_2 [(\dot{x}_2)^2 + (\dot{y}_2)^2] \quad (8)$$

And the potential energy of each mass of the links as:

$$PE = m_1 g L_1 \cos(\theta_1) + m_2 g [L_1 \cos(\theta_1) + L_2 \cos(\theta_1 + \theta_2)] \quad (9)$$

Thus, the Lagrangian formulation to the system as:

$$G = K_E - P_E \quad (10)$$

By using the Euler-Lagrange equation to get both torques τ_1 , and τ_2 by:

$$d/dt (\partial G / \partial \dot{\theta}_i) - \partial G / \partial \theta_i = \tau_i \quad (11)$$

The governing equations of the dynamic system can be written as:

$$\ddot{\theta}_1 = \left(\frac{1}{[(m_1 + m_2)L_2^2 + m_2L_2^2 + 2m_2L_1L_2 \cos \theta_2]} \right) \times \begin{pmatrix} \tau_1 - [m_2L_2^2 + m_2L_1L_2 \cos \theta_2]\ddot{\theta}_2 \\ + 2m_2L_1L_2\dot{\theta}_1\dot{\theta}_2 \sin \theta_2 + m_2L_1L_2S_2\theta_2 \sin \theta_2 \\ - (m_1 + m_2)gL_1 \cos \theta_1 - m_2gL_2 \cos(\theta_1 + \theta_2) \end{pmatrix} \quad (12)$$

$$\ddot{\theta}_2 = \left(\frac{1}{m_2L_2^2} \right) \times \begin{pmatrix} \tau_2 - [m_2L_2^2 + m_2L_1L_2 \cos \theta_2]\ddot{\theta}_1 \\ - m_2L_1L_2\dot{\theta}_1^2 \sin \theta_2 - m_2gL_2 \cos(\theta_1 + \theta_2) \end{pmatrix} \quad (13)$$

In Fig. 2, The implementation of the 2DOF robotic manipulators within the platform environment of MATLAB/Simulink with the suggested controller and Integral Square error (ISE) of a system. The ISE has been computed over a fixed simulation time window of 0 to 20 seconds, with a sampling frequency of 1 kHz to ensure high-resolution error capture.

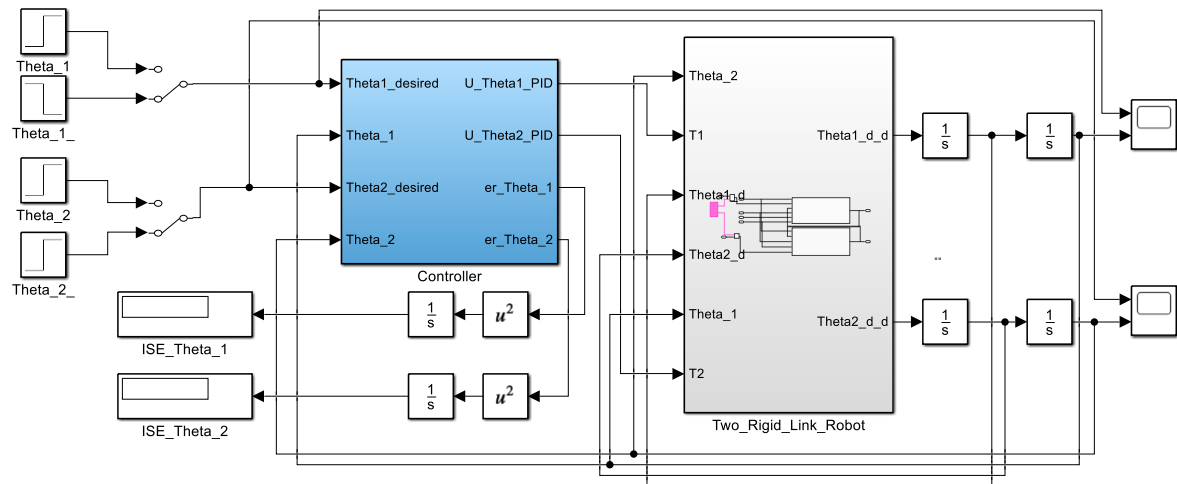


Fig. 2. MATLAB/Simulink model of the proposed 2DOF robotic manipulator

For the purposes of this analysis, each link is assumed to have a mass of 1 kg, and both links are one meter in length. Table 1 provides definitions for the mathematical characters used in the equations that control the system dynamic in (12) and (13).

Table 1. The mathematical characters of the system equations

Description	Characters	The unit
Mass - link1	m1	kg
Mass - link2	m2	kg
Length - link1	L1	m
Length - link2	L2	m
Positions, angular velocities, and accelerations	$\theta_i, \dot{\theta}_i$, and $\ddot{\theta}_i$	rad, rad/s, and rad/s ²
Gravity acceleration	g	kg /m ²
Torques	τ_1 , and τ_2	N. m/rad

2.1. PID Controller

The proportional-integral-derivative (PID) controller is the most commonly used control strategy in industrial processes and automation systems. Although the PID controller helps mitigate the uncertainties within the system dynamics, the overall performance of the dynamic system often remains sluggish and requires further improvement. For both link1 and link2 of the robotic manipulator, the basic structure of the PID controller for any given input can be represented as follows:

The tuning parameters of a PID controller are referred to as the proportional gain (Kp), integral gain (Ki), and derivative gain (Kd). The PID gains were initially tuned using manual refinement through trial-and-error to achieve satisfactory transient and steady-state performance under nominal conditions [6], [23], [38] as follows: for Link 1, Kp = 15, Ki = 0.2, and Kd = 10; for link 2, Kp = 15, Ki = 6.5, Kd = 7.

$$u_1(t) = K_p e(t) + K_i \int e(t) dt + K_d \frac{d}{dt} e(t) \quad (14)$$

$$u_2(t) = K_p e(t) + K_i \int e(t) dt + K_d \frac{d}{dt} e(t) \quad (15)$$

2.2. Sliding Mode Controller (SMC)

Sliding mode approach is a type of nonlinear control method used in control systems. A motion system is forced to follow a desired signal by slipping along a cross-section of its natural behavior by applying a discrete control signal [38], [51]-[52]. This type of slip mode controller, based on hysteresis, imposes on dynamic systems to prevent unwanted deviations in their trajectory. It has been adopted in many motion applications due to its robustness. The sliding-mode index S_{sl} is defined as:

$$S_{sl} = E_{link,p} + \lambda \cdot \dot{E}_{link,p} \quad (16)$$

Where $E_{link,p} = S^* - y(t)$, S^* is the reference set point of the robot link to follow ($\pi/2$) and λ is a positive constant and equal to one. Whilst the $E_{link,p}$ is the error of the link's position, and the $\dot{E}_{link,p}$ is the derivative of the error, and are computed as:

$$\dot{E}_{link,p} = \frac{dE_{link,p}}{dt} \approx \frac{E_{link,p}(k+1) - E_{link,p}(k)}{t_s} \quad (17)$$

Here, the sample time is indicated by t_s . As shown in Fig. 3, the idea of creating a control diagram combines the PID with SMC into an independent control diagram for each arm of the robot to control the movement of the link.

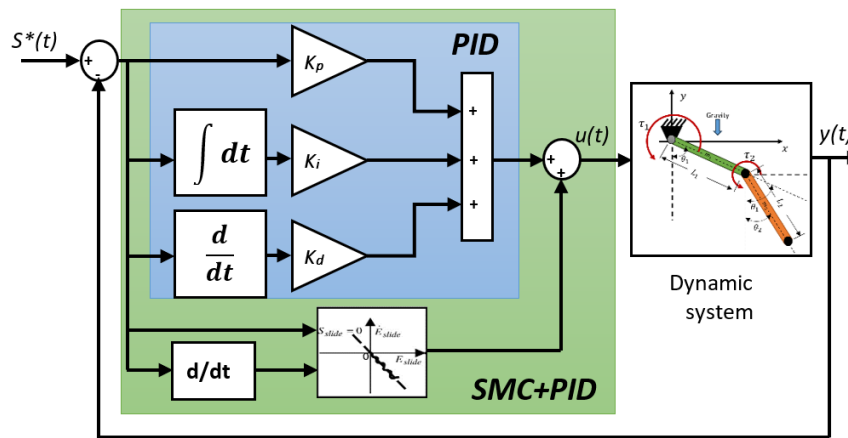


Fig. 3. SMC-PID schematic [38]

2.3. Active Force Control (AFC) Technique

The Principles of the Active Force Control (AFC) strategy is based on real-time force or torque signals obtained from sensors, along with an accurate estimation of the system's inertia. These sensors measure the actual forces or torques generated by the robot's actuators and transmit this data to the control system. In addition to this, AFC can incorporate an error compensation mechanism, which calculates the difference between the desired force and the actual force (known as the force error). The controller then adjusts the actuator inputs accordingly to minimize this error. Through this continuous feedback and correction process, AFC enables dynamic adjustments to maintain the desired force output, even in the presence of external disturbances or environmental changes.

This section presents a method to enhance control performance by merging the PID control signal with the AFC signal. The proposed AFC structure uses the estimated mass or inertia value, along with

the measured acceleration signal, to improve responsiveness and accuracy of the system. As illustrated in Fig. 4, the suggested model integrates the conventional PID defined by the parameters (K_p , K_i , and K_d)- with the AFC technique.

The system utilizes the error signal in a closed-loop manner to identify the system behavior progressively as the error varies over time. Since these signals are accessible in the closed-loop construction of the two-link robotic manipulators, they are employed as input parameters for the controller tuning to enhance system behavior. The estimated disturbance torque (G^*) is derived from the torque in the RR joints of the robot arm, combined with the angular acceleration and the estimated mass (M). This mass estimation can be obtained using either a crude approximation or a precise model [23]-[24]. The disturbance torque (G^*) is then processed through a weighting function $J(s)$, which generates the ultimate AFC signal command to be integrated within an outer control loop and the actuator $T(s)$. The outer control loop employs a proportional-integral-derivative (PID) controller, represented by $u(t)$ as in in (14) and (15), for each robot arm. The PID controller plays a crucial role in enhancing AFC functionality, ensuring robust stability in the two-DOF system.

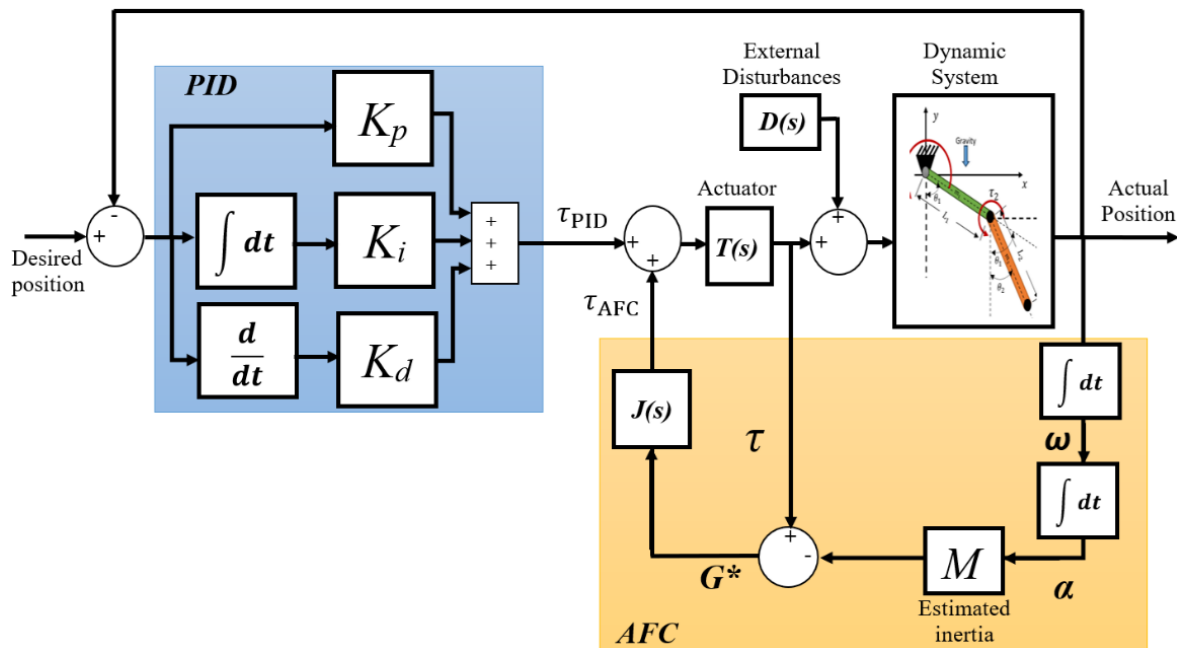


Fig. 4. Coupled scheme of AFC-PID controller

This integrated control approach has been rigorously implemented in numerous AFC-based schemes [4]-[5], [7], [27]-[29], demonstrating its effectiveness in disturbance compensation and system robustness. The following is an expression for the proposed AFC technique:

$$G^* = \tau - \alpha \cdot M \quad (18)$$

$$J(s)T(s) = 1 \quad (19)$$

Where;

τ : Torque

ω : Angular velocity

α : Angular acceleration

G^* : Estimated disturbances torque

M : Estimated inertia

$T(s)$: The actuator

$J(s)$: Weighting function

$D(s)$: External disturbances

The total control torque τ_{total} applied to each joint is composed of two components: the output from the PID controller τ_{PID} and the estimated disturbance compensation torque τ_{AFC} , such that:

$$\tau_{\text{total}} = \tau_{\text{PID}} + \tau_{\text{AFC}} \quad (20)$$

The AFC method aims to reject disturbances by estimating the torque acting on the system. Based on Newton's second law, the estimated disturbance torque τ_{AFC} is computed as:

$$\tau_{\text{AFC}} = M \cdot \alpha - \tau_{\text{measured}} \quad (21)$$

where M is the estimated inertia of the link, α is the measured angular acceleration, and τ_{measured} is the actual actuator torque. This formulation assumes the desired acceleration is approximately equal to the measured acceleration in real time. Research in AFC is focused on improving the robustness and efficiency of control algorithms, integrating artificial intelligence for better adaptability, and developing cost-effective sensors and actuators. Advances in these areas will expand the applications of AFC and enhance the capabilities of robotic and automated systems.

3. Results and Discussion

3.1. Proposed States Results of Passive, PID, and AFC+PID Control Schemes

To compare the behavior of the system starting to display the passive control which is a dynamic system's behavior with no control effect or active feedback. Fig. 5, compares the performance of the two-link robotic manipulator when controlled using a conventional PID controller, SMC-PID, versus the proposed AFC-PID controller. The link1 has a challenging issue to control its position due to the mechanism of carrying the link2. Fig. 5 (a) shows the AFC-PID has the ability to improve the position of the link1 faster and more stable compared with passive and classic PID controllers. The link2 behavior in Fig. 5 (b) also demonstrates shorter and more reliable performance using the proposed approach.

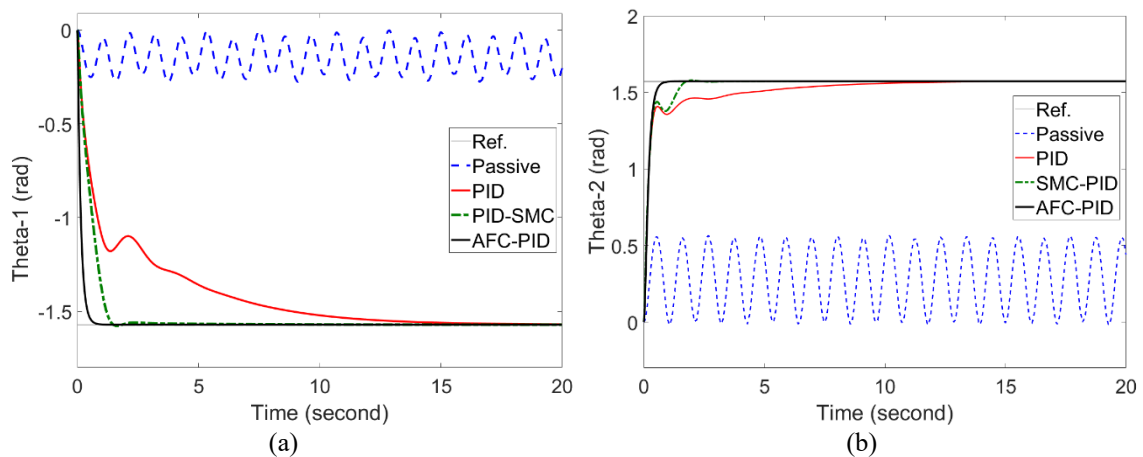


Fig. 5. Systems via AFC-PID, SMC-PID, PID, and Passive: (a) Link's position1 (b) Link's position2

To highlight the effectiveness of the proposed scheme, the response results were compared to those of a PID, and SMC. The contrast was evident with the combined system outperforming the system in suppressing the disturbances associated with the dynamic system.

Table 2 and Table 3 provide the interpretation of the simulated outcomes compare to previous studies. The values for the response parameters' (%) overshoot, rising time, and settling time are listed. The simulation findings show that the AFC-PID controller-equipped system responded faster than the

passive, PID [6], and SMC-PID [38] controllers. Subsequently, the AFC-PID controller minimized overshoot, settling time, and rising time as well as the ISE compare to previous other control performances.

Table 2. Link-1 performance analysis

Link1	Passive	PID [6]	SMC-PID [38]	AFC-PID
Rising Time (s)	Nil	2.7033	0.9842	0.3254
Settling Time (s)	19.98	8.5245	1.3815	0.6239
Overshoot %	12.67	0	0	0
ISE	40.8	1.647	0.3797	0.19

Table 3. Link-2 performance analysis

Link2	Passive	PID [6]	SMC-PID [38]	AFC-PID
Rising Time (s)	Nil	1.0240	1.0633	0.6162
Settling Time (s)	19.98	8.1333	1.5608	1.0760
Overshoot %	12.67	0	0.1232	0
ISE	33.77	0.93	0.323	0.3

3.2. Velocity Results of Passive, PID, and AFC+PID Controllers

All Fig. 6 (a, and b), demonstrates that the required link speeds are significantly greater with the AFC-PID scheme in behavior compared to both passive and PID schemes, then continuing with stable speed. The AFC-PID controller displays superior performance with a fast arm and stable movement.

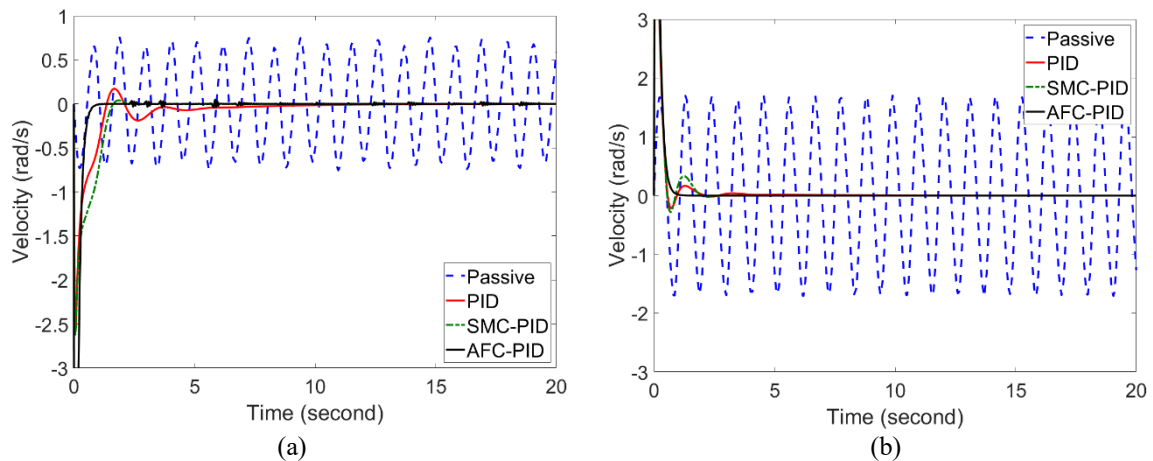


Fig. 6. Velocity analysis via AFC-PID, SMC-PID, PID, and Passive: (a) Link 1's position (b) Link 2's position

3.3. The Robustness of The System Under Disturbances

Only The comparison of the behavior of the RR robot manipulators among Passive, and PID besides the proposed AFC-PID controllers under disturbances [24], [28]. Using the sine wave parameter disturbance leads the system to become inaccurate due to loss of precision and can be considered as an external disturbance. They consider sine wave (5 amplitude, 5 Hz), the band-limited noise with 2.75 intensity limit, and the pulse generator with 5 amplitudes, 2 pulse width. Thus the Fig. 7 (a, b) shows the AFC-PID has robustness toward sine wave disturbances in both link1 and link2 compared to the passive and PID controller.

Table 4 and Table 5 give the interpretation of the simulated results under the disturbances. The indicators of (%) overrun, rising time, and settling time values for the three controller systems are presented to illustrate the behavior of the dynamic system. When compared to the uncertainty behavior of passive control and the presence of the PID controller [6], the AFC-PID controller-based system maintains its robustness with minimum ISE which led to more accurate control performance with proposed control scheme.

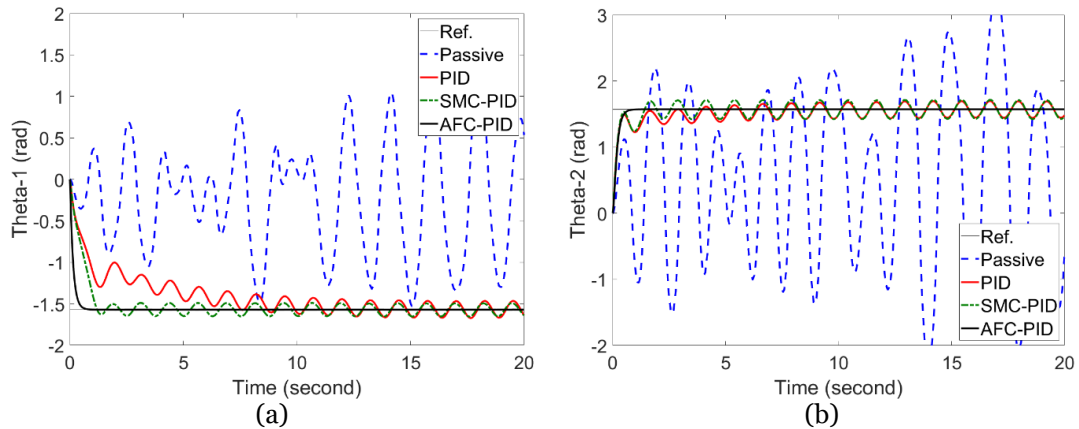


Fig. 7. Controlled the trajectories with sine disturbances: (a) Position of link1. (b) Position of link2

Fig. 8 (a, and b), demonstrates the required link speeds, and they are significantly greater with the AFC-PID scheme in behavior compared to both passive and PID schemes. And when implement deferent disturbances like shown in Fig. 9 (a, b) and Fig. 10 (a, b) the AFC-PID has again robust affect toward pulse generator and band-limited noise disturbances respectively in both link1 and link2 as well as the links speeds in Fig. 11, and Fig. 12 among other controllers. These figures show that the robotic arms speed moves with this proposed strategy more stable than other control schemes. The proposed scheme reduced the resulting oscillations and enhanced response accuracy, and allowing the arm to smoothly reach the desired speed to perform tasks. Also, it reduced settling time and allowed the robotic arm to efficiently adapt to operating loads.

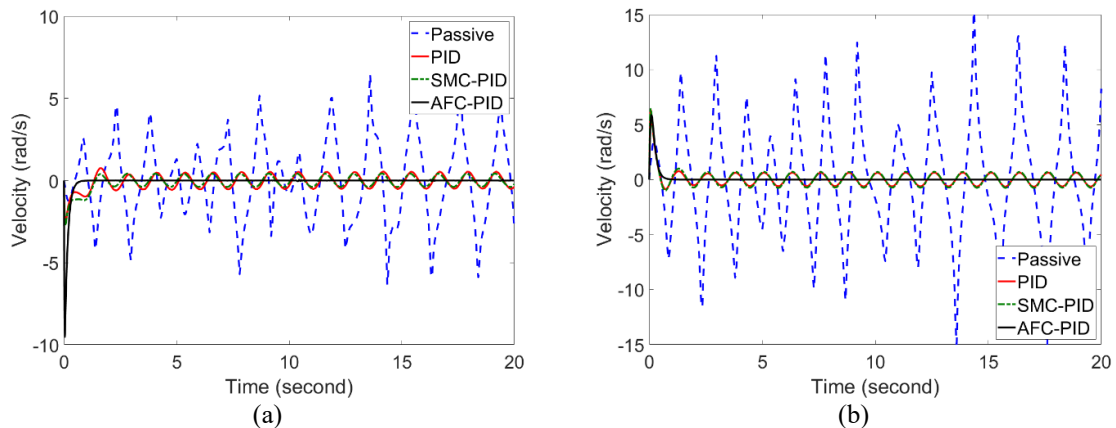


Fig. 8. Velocity analysis with sine disturbances: (a) Link 1's position (b) Link 2's position

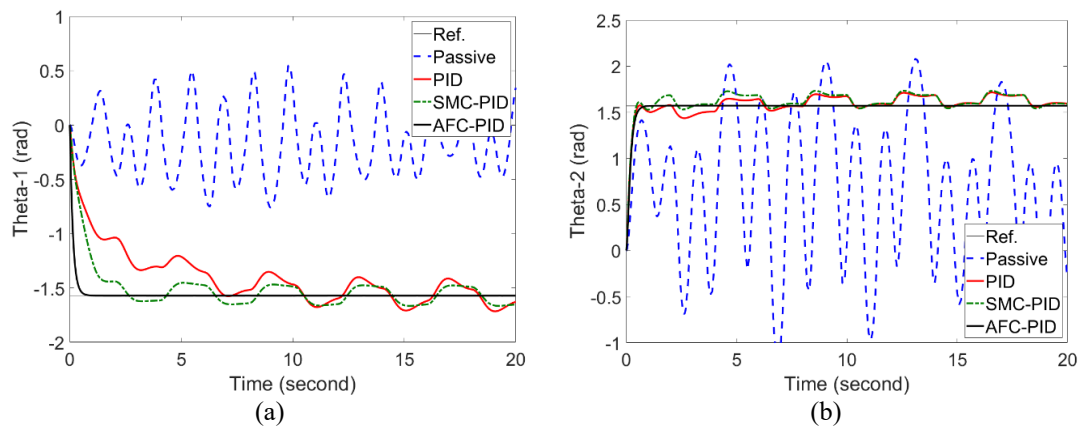


Fig. 9. Controlled the trajectories with pulse generator disturbances: (a) Position of link1. (b) Position of link2

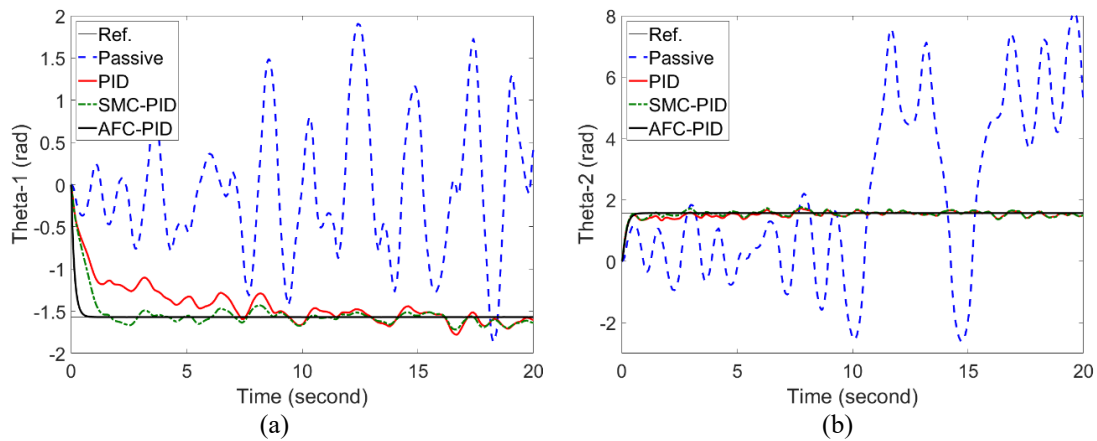


Fig. 10. Controlled the trajectories with band-limited noise with (2.75 intensity) disturbances: (a) Position of link1. (b) Position of link2

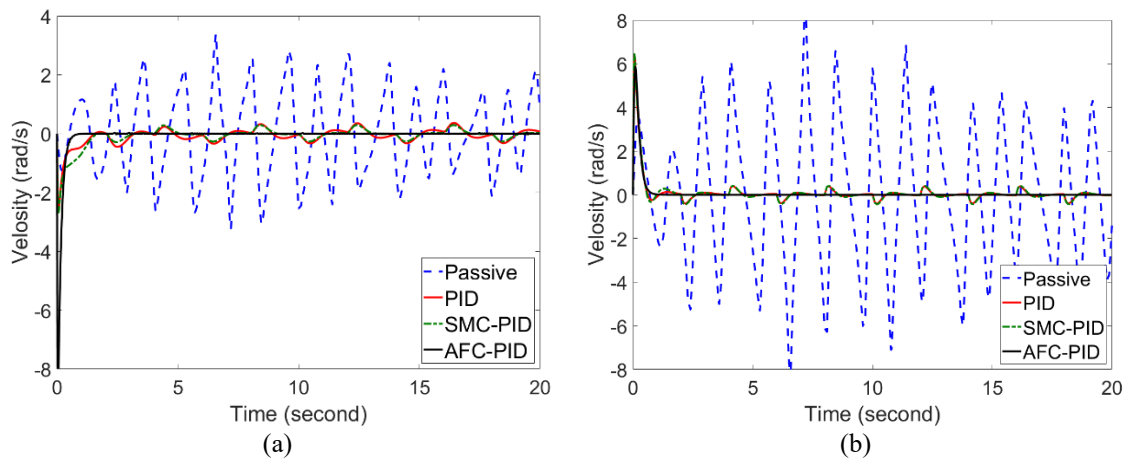


Fig. 11. Velocity analysis under pulse generator disturbances: (a) Position of link1. (b) Position of link2

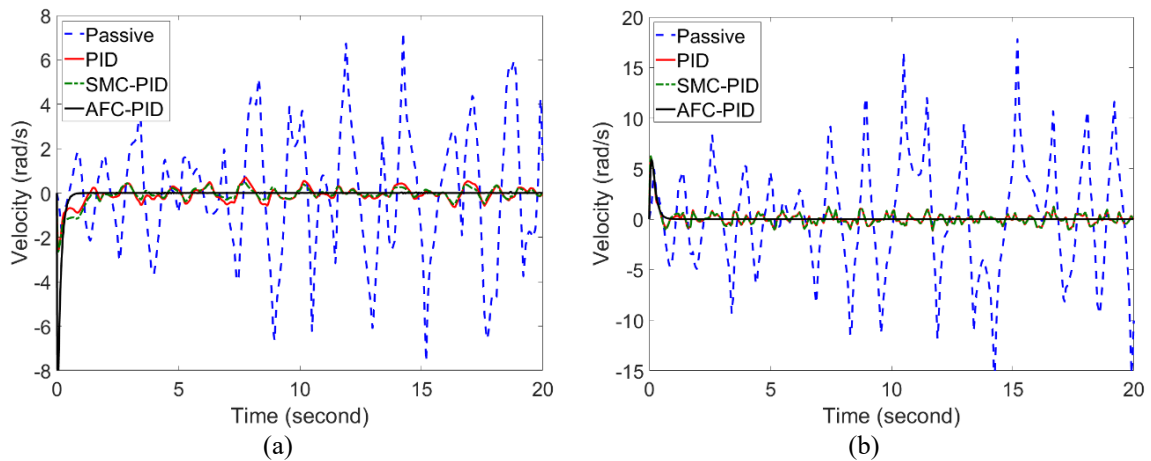


Fig. 12. Velocity analysis under band-limited noise disturbances: (a) Position of link1. (b) Position of link2

Table 4. Link-1 performance analysis under disturbances

Link1	Passive	PID	AFC-PID
Rising Time (s)	Nil	6.32	0.33
Settling Time (s)	19.99	19.59	0.77
Overshoot %	191.26	20.49	0.5
ISE	44.33	2.07	0.2857

Table 5. Link-2 performance analysis under disturbances

Link2	Passive	PID	AFC-PID
Rising Time (s)	6.45	2.58	1.0
Settling Time (s)	19.94	19.23	1.07
Overshoot %	8.83	1.83	0.3
ISE	24.44	0.9238	0.32

4. Conclusions

This study presented a comparative analysis of the AFC-PID controller against conventional PID, SMC-PID, and passive control schemes for a 2-DOF robotic manipulator using MATLAB/Simulink. The evaluation focused on position and velocity at each link. The AFC-PID controller demonstrated superior performance in terms of stability, reduced overshoot, and robustness to external disturbances. It consistently maintained better dynamic behavior under varying conditions, making it suitable for real-time applications. Quantitative analysis using the Integral Squared Error (ISE) metric showed significant improvements: an 82.83% and 65.57% reduction in ISE for Links 1 and 2, respectively, compared to the conventional PID controller. Under external disturbances, the AFC-PID maintained high performance, with ISE improvements of 86.2% and 65.36% for Links 1 and 2. These enhancements are particularly relevant to applications such as surgical robotics, precision manufacturing, and automated assembly, where reliable motion control and disturbance rejection are critical. However, successful implementation requires careful parameter tuning and robustness to noise and response delays. Future work could explore integration with machine learning techniques for real-time parameter identification and adaptive tuning, including the use of empirical estimation methods such as Least Squares (LS) and Recursive Least Squares (RLS).

Author Contribution: All the authors made an equal contribution in this paper. The final manuscript has been reviewed and approved by all authors.

Funding: This research received no external funding.

Acknowledgment: The authors would like to thank the University of Mosul and New Cairo Technological University for their cooperation and scientific support in this study and for completing aspects of this research.

Conflicts of Interest: The authors declare no conflict of interest.

References

- [1] H. Mahdi, S. A. Akgun, S. Saleh, and K. Dautenhahn, "A survey on the design and evolution of social robots: Past, present and future," *Robotics and Autonomous Systems*, vol. 156, p. 104193, 2022, <https://doi.org/10.1016/j.robot.2022.104193>.
- [2] L. Aymerich-Franch and I. Ferrer, "Liaison, safeguard, and well-being: Analyzing the role of social robots during the COVID-19 pandemic," *Technology in Society*, vol. 70, p. 101993, 2022, <https://doi.org/10.1016/j.techsoc.2022.101993>.
- [3] I. M. Alguacil-Diego *et al.*, "A novel active device for shoulder rotation based on force control," *Sensors*, vol. 23, no. 13, p. 6158, 2023, <https://doi.org/10.3390/s23136158>.
- [4] S. Z. Yuan, M. Mailah, and T. H. Hing, "Intelligent Active Force Control of an Underwater Remotely Operated Vehicle Using Evolutionary Computation Technique," *Jurnal Mekanikal*, vol. 43, no. 2, pp. 1-25, 2020, <https://jurnalmekanikal.utm.my/index.php/jurnalmekanikal/article/view/411>.
- [5] M. H. A. Al-Mola, M. Mailah, and M. A. Salim, "Applying active force control with fuzzy self-tuning PID to improve the performance of an antilock braking system," *International Journal of Nanoelectronics and Materials*, vol. 14, pp. 489-502, 2021, [https://ijneam.unimap.edu.my/images/PDF/IJNeaM%20Special%20Issue%202021%20\(1\)/Vol%2014%20SI%20Aug2021%20489-502.pdf](https://ijneam.unimap.edu.my/images/PDF/IJNeaM%20Special%20Issue%202021%20(1)/Vol%2014%20SI%20Aug2021%20489-502.pdf).

- [6] M. H. Al-Mola and S. I. Abdelmaksoud, "Performance Improvement of a Space Robotic Manipulator Using Fuzzy-Based PID Controller," *2023 International Telecommunications Conference (ITC-Egypt)*, pp. 524-529, 2023, <https://doi.org/10.1109/ITC-Egypt58155.2023.10206133>.
- [7] R. Rosli, Z. Mohamed, and G. Priyandoko, "Simulation of active force control using MR damper in semi active seat suspension system," *IOP Conference Series: Materials Science and Engineering*, vol. 1062, no. 1, p. 012005, 2021, <https://doi.org/10.1088/1757-899X/1062/1/012005>.
- [8] B. Huo, R. Wang, Y. Qin, Z. Wu, G. Bian, and Y. Liu, "Force tracking control of functional electrical stimulation via hybrid active disturbance rejection control," *Electronics*, vol. 11, no. 11, p. 1727, 2022, <https://doi.org/10.3390/electronics11111727>.
- [9] K. Bodie *et al.*, "Active Interaction Force Control for Contact-Based Inspection With a Fully Actuated Aerial Vehicle," *IEEE Transactions on Robotics*, vol. 37, no. 3, pp. 709-722, 2021, <https://doi.org/10.1109/TRO.2020.3036623>.
- [10] N. M. Trieu and N. T. Thinh, "Enhancing emotional expressiveness in biomechanics robotic head: A novel fuzzy approach for robotic facial skin's actuators," *Computer Modeling in Engineering & Sciences*, vol. 143, no. 1, pp. 477-498, 2025, <https://doi.org/10.32604/cmes.2025.061339>.
- [11] N. Gupta and B. Pratiher, "Dynamic modeling and effective vibration reduction of dual-link flexible manipulators with two-stage cascade PID and active torque actuation," *Mechanism and Machine Theory*, vol. 205, p. 105867, 2025, <https://doi.org/10.1016/j.mechmachtheory.2024.105867>.
- [12] J. Li, "Analysis and Comparison of Different Tuning Method of PID Control in Robot Manipulator," *Highlights in Science, Engineering and Technology*, vol. 71, pp. 28-36, 2023, <https://doi.org/10.54097/hset.v71i.12373>.
- [13] M. Mohsen, A. M. Mohamed, S. M. Ahmed, and K. Ibrahim, "Bilateral control of a 2-DOF teleoperated manipulator using UDP scheme," *Ain Shams Engineering Journal*, vol. 14, no. 9, p. 102065, 2023, <https://doi.org/10.1016/j.asej.2022.102065>.
- [14] W. Faris, M. Rabie, A. Moaaz, N. Ghazaly, and M. Makrahy, "Two-flexible-link manipulator vibration reduction through fuzzy-based position," *International Journal of Robotics and Control Systems*, vol. 5, no. 1, pp. 479-499, 2025, <https://doi.org/10.31763/ijrcs.v5i1.1669>.
- [15] H. R. Nohooji, A. Zaraki, and H. Voos, "Actor-critic learning based PID control for robotic manipulators," *Applied Soft Computing*, vol. 151, p. 111153, 2024, <https://doi.org/10.1016/j.asoc.2023.111153>.
- [16] G. Ahmed, A. Eltayeb, N. M. Alyazidi, I. H. Imran, T. Sheltami, and S. El-Ferik, "Improved particle swarm Optimization for fractional Order PID control design in Robotic Manipulator System: A Performance analysis," *Results in Engineering*, vol. 24, p. 103089, 2024, <https://doi.org/10.1016/j.rineng.2024.103089>.
- [17] R. Kumar and K. Kumar, "Design and control of a two-link robotic manipulator: A review," *AIP Conference Proceedings*, vol. 2358, no. 1, p. 050020, 2021, <https://doi.org/10.1063/5.0057931>.
- [18] K. K. Lin, A. K. Soe, and T. T. Thu, "Fuzzy control of robotic arm," *AIP Conference Proceedings*, vol. 1052, no. 1, pp. 147-150, 2008, <https://doi.org/10.1063/1.3008659>.
- [19] A. A. Mohammed and A. Eltayeb, "Dynamics and Control of a Two-link Manipulator using PID and Sliding Mode Control," *2018 International Conference on Computer, Control, Electrical, and Electronics Engineering (ICCCEEE)*, pp. 1-5, 2018, <https://doi.org/10.1109/ICCCEEE.2018.8515795>.
- [20] M. H. Al-Mola and M. A. B. Salim, "Improving the performance of pipeline petrol-transportation using fuzzy logic control based PID tuning," *International Journal of Engineering and Applied Sciences*, vol. 12, no. 5, p. 299, 2024, <https://doi.org/10.15866/irea.v12i5.23651>.
- [21] W. Alqaisi, M. Soliman, A. Badawi, I. Elzein, and C. El-Bayeh, "Four DOF robot manipulator control using feedback linearization based on sliding mode control," *International Journal of Robotics and Control Systems*, vol. 5, no. 2, pp. 781-793, 2025, <https://doi.org/10.31763/ijrcs.v5i2.1729>.
- [22] Manjeet and Sathans, "Fuzzy Based Control of Two Link Robotic Manipulator and Comparative Analysis," *2013 International Conference on Communication Systems and Network Technologies*, pp. 562-567, 2013, <https://doi.org/10.1109/CSNT.2013.121>.

-
- [23] M. H. Al-Mola, M. Mailah, and S. I. Abdelmaksoud, "Experimental implementation of a vehicle anti-lock brake system employing intelligent active force control with a P-type iterative learning algorithm," *Transactions of the Institute of Measurement and Control*, vol. 45, no. 13, pp. 2554-2565, 2023, <https://doi.org/10.1177/01423312231156960>.
- [24] C. E. Martínez-Ochoa, I. O. Benítez-González, A. O. Cepero-Díaz, J. R. Nuñez-Alvarez, C. G. Miguélez-Machado, and Y. E. Llosas-Albuérne, "Active disturbance rejection control for robot manipulator," *Journal of Robotics and Control*, vol. 3, no. 5, pp. 622-632, 2022, <https://doi.org/10.18196/jrc.v3i5.14791>.
- [25] J. Dai, C.-Y. Chen, R. Zhu, G. Yang, C. Wang, and S. Bai, "Suppress Vibration on Robotic Polishing with Impedance Matching," *Actuators*, vol. 10, no. 3, p. 59, 2021, <https://doi.org/10.3390/act10030059>.
- [26] C. C. Beltran-Hernandez *et al.*, "Learning Force Control for Contact-Rich Manipulation Tasks With Rigid Position-Controlled Robots," *IEEE Robotics and Automation Letters*, vol. 5, no. 4, pp. 5709-5716, 2020, <https://doi.org/10.1109/LRA.2020.3010739>.
- [27] Y. J. W. Lee and Q. Pham, "Robotic assembly across multiple contact stiffnesses with robust force controllers," *ArXiv*, 2020, <https://doi.org/10.48550/arXiv.2003.03047>.
- [28] S. H. Sheng and M. Mailah, "Active Force Control of An Inverted Pendulum: Simulation and Experimental Implementation," *Jurnal Mekanikal*, vol. 41, no. 2-S, pp. 67-79, 2019, <https://jurnalmekanikal.utm.my/index.php/jurnalmekanikal/article/view/343>.
- [29] H. Chen, J. Yang, and H. Ding, "Robotic compliant grinding of curved parts based on a designed active force-controlled end-effector with optimized series elastic component," *Robotics and Computer-Integrated Manufacturing*, vol. 86, p. 102646, 2024, <https://doi.org/10.1016/j.rcim.2023.102646>.
- [30] X. Meng, H. Yu, H. Wu, and T. Xu, "Disturbance Observer-Based Integral Backstepping Control for a Two-Tank Liquid Level System Subject to External Disturbances," *Mathematical Problems in Engineering*, vol. 2020, no. 1, pp. 1-22, 2020, <https://doi.org/10.1155/2020/6801205>.
- [31] P. Ordaz, L. Rodríguez-Guerrero, M. Ordaz-Oliver, and B. Sánchez, "Three link flexible arm robust regulation via proportional retarded control scheme," *Applied Mathematical Modelling*, vol. 125, pp. 778-797, 2024, <https://doi.org/10.1016/j.apm.2023.10.029>.
- [32] S. K. Jagatheesaperumal, V. P. Rajamohan, A. Daud, A. Bukhari, and O. Alghushairy, "QCASBC: An algorithm for hardware-in-the-loop simulation of 3-link RRR robotic manipulator," *Alexandria Engineering Journal*, vol. 103, pp. 12-20, 2024, <https://doi.org/10.1016/j.aej.2024.05.092>.
- [33] T. Wang, Y. Xia, K. Zhao, W. Ning and W. Zhao, "Fixed-Time Disturbance Rejection Control Scheme for Quadrotor Trajectory Tracking," *IEEE Transactions on Industrial Electronics*, pp. 1-11, 2025, <https://doi.org/10.1109/TIE.2025.3531489>.
- [34] D. Sain, B. M. Mohan, and J.-M. Yang, "Development of a 2-DoF nonlinear fuzzy PI-PD controller for a tractor active suspension system," *Computers and Electronics in Agriculture*, vol. 232, p. 110076, 2025, <https://doi.org/10.1016/j.compag.2025.110076>.
- [35] Z. Li and D. Huang, "Robust control of two-link manipulator with disturbance torque and time-varying mass loads," *Transactions of the Institute of Measurement and Control*, vol. 42, no. 9, pp. 1667-1674, 2020, <https://doi.org/10.1177/0142331219894413>.
- [36] K. C. Rath, S. Sahu, A. Nayak, S. Pradhan, G. A. Sharma, and P. P. Munibara, "Geometrical significance of trajectory planning through polynomial equation-Customized RPPRR model robot," *AIP Conference Proceedings*, vol. 2477, no. 1, p. 020001, 2023, <https://doi.org/10.1063/5.0155187>.
- [37] O. Zhang *et al.*, "Trajectory optimization and tracking control of free-flying space robots for capturing non-cooperative tumbling objects," *Aerospace Science and Technology*, vol. 143, p. 108718, 2023, <https://doi.org/10.1016/j.ast.2023.108718>.
- [38] M. H. A. Al-Mola and S. I. Abdelmaksoud, "Trajectory behavior of Two-Link Manipulators using Sliding Mode Control based PID," *2024 1st International Conference on Innovative Engineering Sciences and Technological Research (ICIESTR)*, pp. 1-6, 2024, <https://doi.org/10.1109/ICIESTR60916.2024.10798134>.
-

-
- [39] Y. Shen, "Robotic trajectory tracking control system based on fuzzy neural network," *Measurement: Sensors*, vol. 31, p. 101006, 2024, <https://doi.org/10.1016/j.measen.2023.101006>.
- [40] X. Wang and J. Katupitiya, "Robust control of a dual-arm space robot to capture a non-cooperative target in 3D space," *Aerospace Science and Technology*, vol. 141, p. 108538, 2023, <https://doi.org/10.1016/j.ast.2023.108538>.
- [41] M. J. Mohamed, B. K. Oleiwi, A. T. Azar, and I. A. Hameed, "Coot optimization algorithm-tuned neural network-enhanced PID controllers for robust trajectory tracking of three-link rigid robot manipulator," *Heliyon*, vol. 10, no. 13, p. e32661, 2024, <https://doi.org/10.1016/j.heliyon.2024.e32661>.
- [42] R. M. Mahamood, "Adaptive Controller Design for Two-Link Flexible Manipulator," *IAENG Transactions on Engineering Technologies*, pp. 115-128, 2013, https://doi.org/10.1007/978-94-007-6818-5_9.
- [43] L. Angel and J. Viola, "Control Performance Assessment of Fractional-Order PID Controllers Applied to Tracking Trajectory Control of Robotic Systems," *WSEAS Transactions on Systems and Control*, vol. 17, pp. 62-73, 2022, <https://doi.org/10.37394/23203.2022.17.8>.
- [44] N. T. Minh Nguyet and D. X. Ba, "A neural flexible PID controller for task-space control of robotic manipulators," *Frontiers in Robotics and AI*, vol. 9, p. 975850, 2023, <https://doi.org/10.3389/frobt.2022.975850>.
- [45] A. Ghediri, K. Lamamra, A. Ait Kaki, and S. Vaidyanathan, "Adaptive PID computed-torque control of robot manipulators based on DDPG reinforcement learning," *International Journal of Modelling, Identification and Control*, vol. 41, no. 3, pp. 173-185, 2022, <https://doi.org/10.1504/IJMIC.2022.127518>.
- [46] W. Di, L. Bei, N. Chengbo and Y. Yang, "Anti-disturbance PID attitude tracking control for robotic manipulators via DOBC approach," *2018 33rd Youth Academic Annual Conference of Chinese Association of Automation (YAC)*, pp. 983-987, 2018, <https://doi.org/10.1109/YAC.2018.8406514>.
- [47] G. Sun, Q. Liu, F. Pan, and J. Zheng, "Disturbance observer based adaptive predefined-time sliding mode control for robot manipulators with uncertainties and disturbances," *International Journal of Robust and Nonlinear Control*, vol. 34, no. 18, pp. 12349-12374, 2024, <https://doi.org/10.1002/rnc.7628>.
- [48] K. Merckaert, B. Convens, C. J. Wu, A. Roncone, M. M. Nicotra, and B. Vanderborght, "Real-time motion control of robotic manipulators for safe human-robot coexistence," *Robotics and Computer-Integrated Manufacturing*, vol. 73, p. 102223, 2022, <https://doi.org/10.1016/j.rcim.2021.102223>.
- [49] X. Jia, J. Yang, K. Lu, Y. Pan and H. Yu, "Enhanced Robust Motion Control based on Unknown System Dynamics Estimator for Robot Manipulators," *2024 IEEE International Conference on Robotics and Automation (ICRA)*, pp. 3514-3519, 2024, <https://doi.org/10.1109/ICRA57147.2024.10611460>.
- [50] Y. Yang, H. Xu and X. Yao, "Disturbance Rejection Event-Triggered Robust Model Predictive Control for Tracking of Constrained Uncertain Robotic Manipulators," *IEEE Transactions on Cybernetics*, vol. 54, no. 6, pp. 3540-3552, 2024, <https://doi.org/10.1109/TCYB.2023.3305941>.
- [51] A. Eltayeb, M. F. Rahmat, M. A. M. Eltoum, S. Ibrahim M. H. and M. A. M. Basri, "Adaptive sliding mode control design for the 2-DOF robot arm manipulators," *2019 International Conference on Computer, Control, Electrical, and Electronics Engineering (ICCCEEE)*, pp. 1-5, 2019, <https://doi.org/10.1109/ICCCEEE46830.2019.9071314>.
- [52] B. Kharabian and H. Mirinejad, "Hybrid Sliding Mode/H-Infinity Control Approach for Uncertain Flexible Manipulators," *IEEE Access*, vol. 8, pp. 170452-170460, 2020, <https://doi.org/10.1109/access.2020.3024150>.
-